

Communication

Application of CO₂-Assisted Polymer Compression to Polylactic Acid and the Relationship between Crystallinity and Plasticization

Takafumi Aizawa 

Research Institute for Chemical Process Technology, National Institute of Advanced Industrial Science and Technology, 4-2-1 Nigatake, Miyagino-ku, Sendai 983-8551, Japan; t.aizawa@aist.go.jp; Tel.: +81-22-237-5211

Abstract: CO₂-assisted polymer compression (CAPC) is an environmentally friendly processing method that uses CO₂ to plasticize and crimp polymer fibers at room temperature, enabling low-energy processing within a short time. In this study, CAPC was applied to polylactic acid (PLA), a carbon-neutral polymer. To evaluate the relationships between CO₂ plasticization and the crystallinity degree and plasticization of PLA, samples with different degrees of crystallinity were layered and simultaneously compressed to observe the most collapsed layer. The sample with lower crystallinity exhibited better crushing and higher plasticization than the crystallized samples. The PLA with high crystallinity developed cracks on the fiber surfaces with consequent loss of strength. Based on the results, CAPC is a potentially effective method for PLA with low crystallinity.

Keywords: CO₂-assisted polymer compression; polylactic acid; crystallinity; plasticization



Citation: Aizawa, T. Application of CO₂-Assisted Polymer Compression to Polylactic Acid and the Relationship between Crystallinity and Plasticization. *Compounds* **2021**, *1*, 75–82. <https://doi.org/10.3390/compounds1020007>

Academic Editor: Serena Coiai

Received: 7 June 2021

Accepted: 21 July 2021

Published: 4 August 2021

Publisher's Note: MDPI stays neutral with regard to jurisdictional claims in published maps and institutional affiliations.



Copyright: © 2021 by the author. Licensee MDPI, Basel, Switzerland. This article is an open access article distributed under the terms and conditions of the Creative Commons Attribution (CC BY) license (<https://creativecommons.org/licenses/by/4.0/>).

1. Introduction

Reducing the use of fossil resources is an integral part of building a sustainable society, and has become a challenge in the twenty-first century. Indeed, fossil-fuel alternatives were declared as a sustainable development goal at the UN Summit in September 2015 [1]. Plastics, an indispensable material in our daily lives, must also be converted to plant-based plastics [2]. Polylactic acid (PLA) has the largest production volume among the current bioplastics [3]. As PLA is produced on commercial scales, its handling, processing, and applications have been extensively researched [4]. As an example of PLA application, active food packaging has been proposed [5,6].

The CO₂-assisted polymer compression (CAPC) method fabricates plastic parts at low cost and low energy using CO₂ [7]. In the CAPC method, polymer fibers are placed in a mold and compressed while CO₂ is added. The polymer fibers plasticized by CO₂ are pressed and bonded into porous materials. It can be regarded as a CO₂ capture and utilization (CCU) method [8] because it uses CO₂ as a plasticizer. The porous materials prepared by this new method have been studied in porosity control [9], adhesion strength [10], gas permeability [11], drug release [12], mass production [13], and multilayering [14,15] studies. Past studies of plasticization by CO₂ have suggested that CO₂ impregnates the amorphous part of resins [16–18], but the relationship between the crystallinity of raw materials and their suitability for CAPC processes remains unclear. The combination of CO₂ and PLA has been considered as a suitable sustainable method [19,20].

The pores in a CAPC product are the gaps between the fibers. The CAPC proceeds at room temperature under vapor pressure CO₂ and does not require heaters or pumps. Therefore, CAPC is a very energy-efficient process. In addition, as CO₂ is lowly toxic, it can be applied to pharmaceutical manufacturing and as a food additive in the food industries [21]. The porous material produced by the CAPC method has already demonstrated its potential as a filter and drug-releasing tablet [11,12]. CAPC is a technology for molding porous resins with continuous pores, and it is expected that PLA will be used in many applications, such as filters, catalyst-loaded reactors, and drug capsules.

In previous work, the CAPC method was applied to polyethylene terephthalate [9–15]. In the present study, the CAPC method is newly applied to PLA as an environmentally friendly processing method on an environmentally friendly resin. The effect of the crystallinity of raw fibers on CAPC processes was discussed to determine if there are any restrictions on using raw materials from the viewpoint of crystallinity.

2. Materials and Methods

The raw materials were PLA pellets (Luminy L105, Melt flow index 70 g/10 min (210 °C, 2.16 kg), Total Corbion PLA, Rayong, Thailand), and the nonwoven fabric (fiber diameter = 8 µm) was manufactured by Nippon Nozzle Co., Ltd. (Kobe, Japan) using the melt blowing method [22] with a 0.3-mm nozzle.

To control the crystallization degree of the nonwoven fabrics, the prepared nonwoven fabrics were heated at 62 °C for different times (1, 3, and 10 h). The heating temperature was only slightly higher than the glass transition point (60 °C in the data sheet).

To clarify the order of plasticization in the presence of CO₂, an experiment was conducted in which two samples were stacked, set in a high-pressure vessel, and then pressed. In single experiment, the order of plasticization of the two samples in the same environment could be determined, and the order of plasticization of all samples could be determined by experimenting with different combinations of samples. The untreated, 1-h-treated, 3-h-treated, and 10-h-treated nonwoven fabrics were punched with a Φ-18-mm punch. The experimental setup is shown in Figure 1. CO₂ lines were connected to the piston, and a pressure vessel was placed below the piston. Valves V₁ to V₃ are ball valves, and valve V₄ is a metering valve. Stacked 32 circular sheets (18-mm diameter, 0.253 g) were prepared on the upper and lower sides of the separator and placed in a high-pressure vessel (20-mm inner diameter). After lowering the piston to the CO₂ introduction position (where the total of the upper and lower layers was 3.6 mm), the entry–exhaust cycle of CO₂ was performed three times through valves V₁ and V₂ to drive out the air in the vessel. After replacing air with CO₂, valve V₁ was opened to introduce gaseous CO₂ at vapor pressure (~6 MPa), and the piston was lowered to the press position (where the total of the upper and lower layers was 2.4 mm), where it was held for 10 s. Next, exhaust valve V₃ was opened and exhausted for 30 s through the flow-limiting valve V₄. Finally, V₂ valve was opened to release CO₂ to the atmosphere, and the piston was raised to remove the samples. The experiment was conducted at room temperature (~22 °C) and no heating manipulation was used. The thickness of the center of each sample was measured with a micrometer caliper.

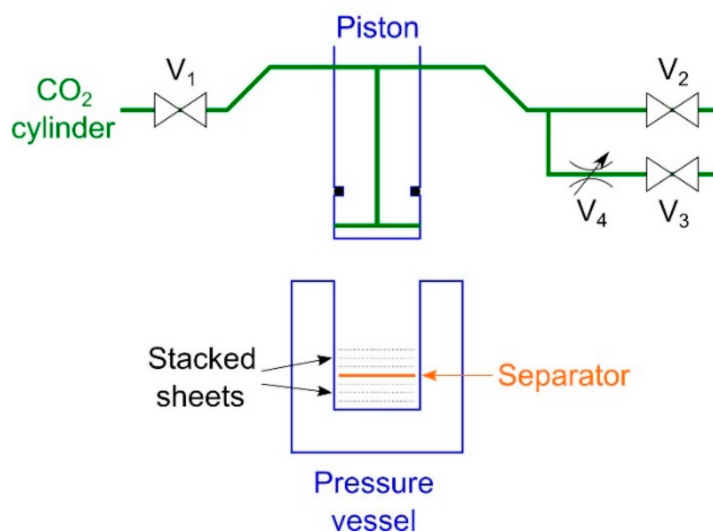


Figure 1. Setup of the experiment for comparing the hardness values of the two layers (V₁: CO₂ introduction valve, V₂: fast exhaust valve, V₃: slow exhaust valve, V₄: metering valve).

To determine the crystallinity degree of each sample, the heat of crystallization was evaluated from differential scanning calorimetry (DSC) measurements conducted on a Thermo Plus Evo DSC 8230 (Rigaku Corporation, Akishima, Japan). The thermograms were recorded under the atmosphere. The heating rate was 5 °C/min. The sample mass was in the range of 7.5–9.1 mg. Melting and crystallization characteristics were evaluated from the first heating run. X-ray diffraction (XRD) patterns were obtained using a SmartLab diffractometer (Rigaku Corporation, Akishima, Japan). The degree of crystallinity was calculated from the cold crystallization and melting enthalpy.

The surface of the CAPC products was observed in a TM-1000 scanning electron microscope (SEM) system (Hitachi High-Technologies Co., Minato-ku, Japan).

3. Results and Discussion

First, I checked whether PLA fibers could adhere using CAPC. The experiments were conducted on untreated sheets. Sixteen sheets with punch diameters of 30 mm were CAPC-treated to form 0.6-mm-thick sheet-like samples. Figure 2 displays photographs of raw nonwoven fabric sheets, the sample after cutting with scissors, and the sample after cutting and bending. The samples were firmly bonded without peeling, indicating the effectiveness of PLA processing by CAPC. In an attempted T-type tensile test, configured by inserting a central sheet to create a non-adhesive area, the sheet sample exhibited higher adhesive strength than the raw fiber; accordingly, the sheet was torn and could not be tested (Figure 3). Therefore, the adhesive strength of the fiber sheets was very high.

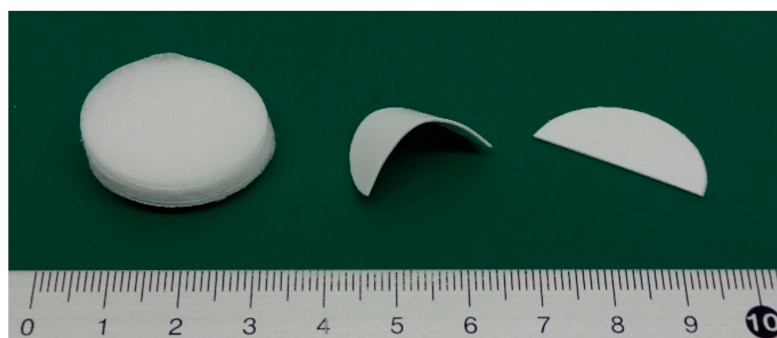


Figure 2. Raw nonwoven fabric sheets (left), a cut and bent CAPC product (middle), and a cut CAPC product (right).

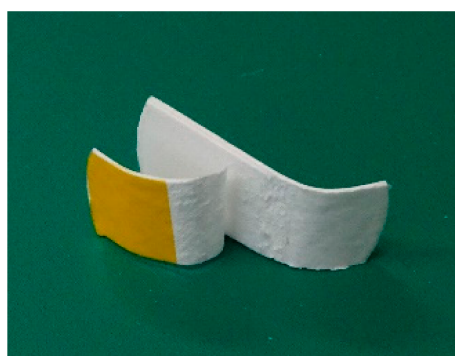


Figure 3. Sample after the T-type tensile test.

Next, the degree of plasticization was evaluated in the presence of CO₂ and was related to the degree of crystallinity. Figure 4 shows the DSC data for each sample; the DSC chart shows the peaks of cold crystallization 1, cold crystallization 2, and fusion at ~93 °C, ~157 °C, and ~174 °C, respectively, similar to an existing study [23]. The enthalpies of cold crystallization 1, cold crystallization 2, and fusion are ΔH_c^1 , ΔH_c^2 , and

ΔH_m , respectively, and considering their signs, the degree of crystallinity is given by the following equation [24]:

$$\text{Degree of Crystallinity} = \frac{\Delta H_c^1 + \Delta H_c^2 + \Delta H_m}{\Delta H_0} \quad (1)$$

where ΔH_0 is the heat of fusion when the crystallinity degree of PLA is 100%, which is -93.1 J/g [25]. Because an overlap exists between the cold crystallization 2 and melting peaks, the integrated values of both were evaluated and analyzed by transforming Equation (1) into the following equation:

$$\text{Degree of Crystallinity} = \frac{\Delta H_c^1 + \Delta H_{c+m}^2}{\Delta H_0} \quad (2)$$

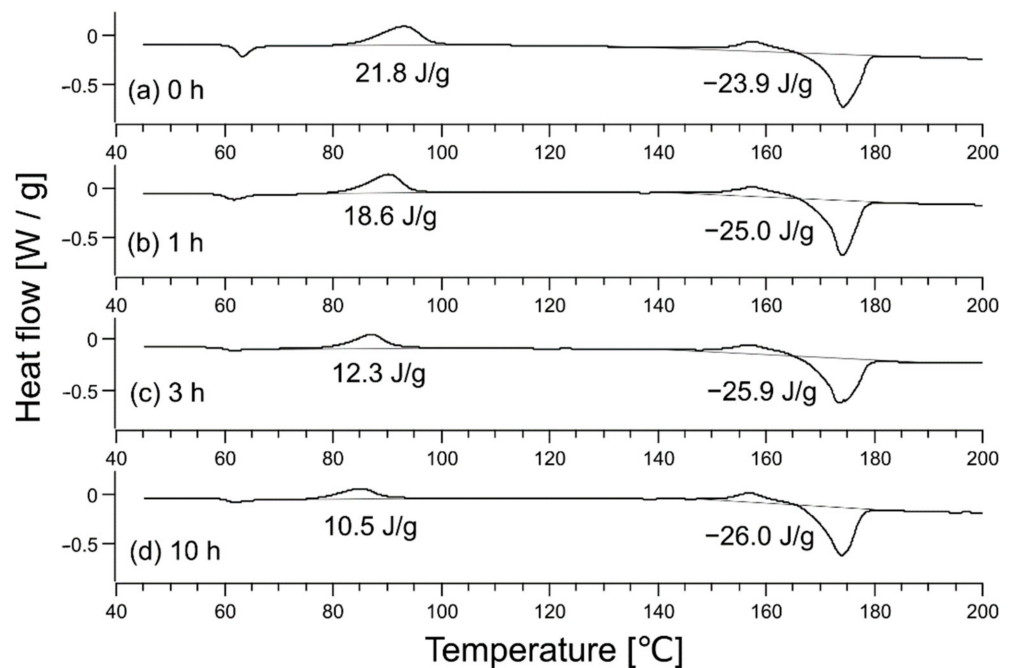


Figure 4. Differential scanning calorimetry data of (a) a raw fabric sheet and the sheet after heating at 62 °C for different times: (b) 1 h, (c) 3 h, and (d) 10 h. Indicated values are enthalpies of ΔH_c^1 and ΔH_{c+m}^2 in Equation (2).

Derived crystallinities were 0.02 (unheated), 0.07 (1-h heating), 0.15 (3-h heating), and 0.17 (10-h heating).

XRD data of unheated nonwoven fabric is shown in Figure 5. The degree of crystallinity is calculated as the area ratio of the broad halo due to the amorphous part and the sharp peak due to the crystalline part in the XRD data [26]. The XRD chart in Figure 5 shows no sharp peaks, and the degree of crystallinity was almost zero, which agreed with the value calculated from DSC data (0.02).

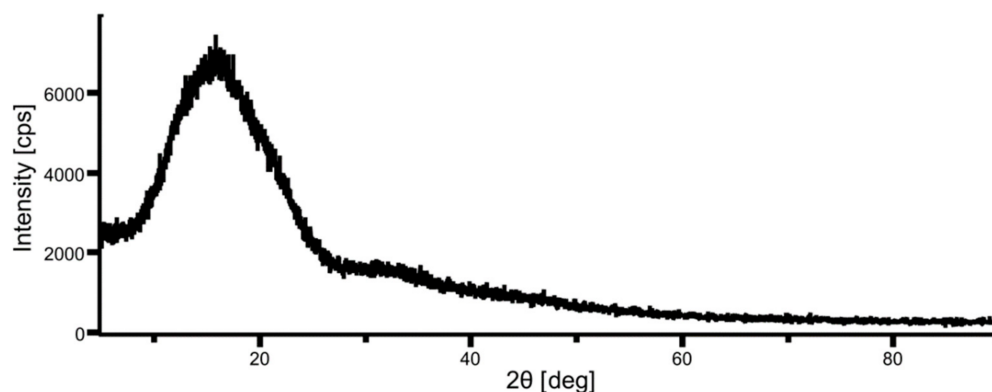


Figure 5. XRD data of a raw fabric sheet.

To analyze the hardness of the samples impregnated with CO_2 , a separator was placed between the two samples, and the entire sample was compressed to a certain thickness. The raw material comprises stacked nonwoven fabrics, and the product is a uniform porous material with a certain thickness. The thicknesses of the CAPC products above and below the separator were measured to determine their relative hardness.

First, untreated samples were set at both the top and bottom, and they were then compressed to a total of 2.4 mm. The experiments were performed four times. CAPC products were formed at the top and bottom through the separator. The top and bottom CAPC products were of the same thickness (1.200 ± 0.002 mm), confirming that the samples were compressed in the same manner regardless of their position. Next, experiments with six different sample combinations were performed; the experiments were performed four times in each combination. Two experiments were conducted with sample A on the top and sample B on the bottom, and the other two were conducted with sample A on the bottom and sample B on the top. Then, the results of these experiments were averaged and demonstrated, as shown in Table 1. The sample name indicates the experiment number (samples A and B in each experiment). For example, experiment number 1 is a combination of an untreated sample and a 1-h-heated sample, where the untreated sample is 1A and the 1-h-heated one is 1B. Comparing the untreated and 1-h-heated samples, the untreated sample was more crushed, indicating that the sample without heat treatment was more plasticized by CO_2 . The untreated sample crumbled more as its counterpart was heated for longer times, indicating that it hardened after heating for 3 h and further hardened after 10 h. This result indicates that the degree of crystallization increased with heating time, inhibiting the plasticization effect of CO_2 . In fact, the 1-h-heated sample was more compressed than the 3-h-heated sample, and the 3-h-heated sample was more compressed than the 10-h-heated sample. In summary, the hardening increased in the following order: untreated < 1-h heating < 3-h heating < 10-h heating. CO_2 plasticizes polymers by dissolving in the amorphous part of the polymers [27,28]. The results in this study show that the hardness of the polymer in CO_2 increases as the amorphous part decreases, which is consistent with previous studies.

Table 1. Compression results for the hardness comparison.

Sample	Heat-Treatment Time [h]	Thickness [mm]	Standard Deviation [mm]
1A	0	1.197	0.003
1B	1	1.206	0.003
2A	0	1.152	0.018
2B	3	1.249	0.019
3A	0	1.114	0.006
3B	10	1.285	0.005
4A	1	1.157	0.004
4B	3	1.246	0.009
5A	1	1.140	0.009
5B	10	1.261	0.009
6A	3	1.173	0.010
6B	10	1.229	0.006

The untreated samples bonded very well, but the 10-h-heated sample appeared brittle. Therefore, the microscopic surface morphologies of the samples were compared. Figure 6 compares the SEM images of the sample surfaces after the CAPC process. In the untreated CAPC product, the fibers were crushed and spread horizontally by the plasticization and pressing processes, but this crushing was increasingly reduced as the heat treatment progressed. In addition, the fibers in the 10-h-heated product were cracked and fiber damage was confirmed. The flexural strength and maximum strain of PLA, whose crystallinity is increased through annealing, decreases owing to the rigidity effects of the crystalline domains [4,23]. These effects must have appeared in the cracks in the 10-h-heated product. Therefore, the CAPC method should be limited to PLA fibers with low crystallinity.

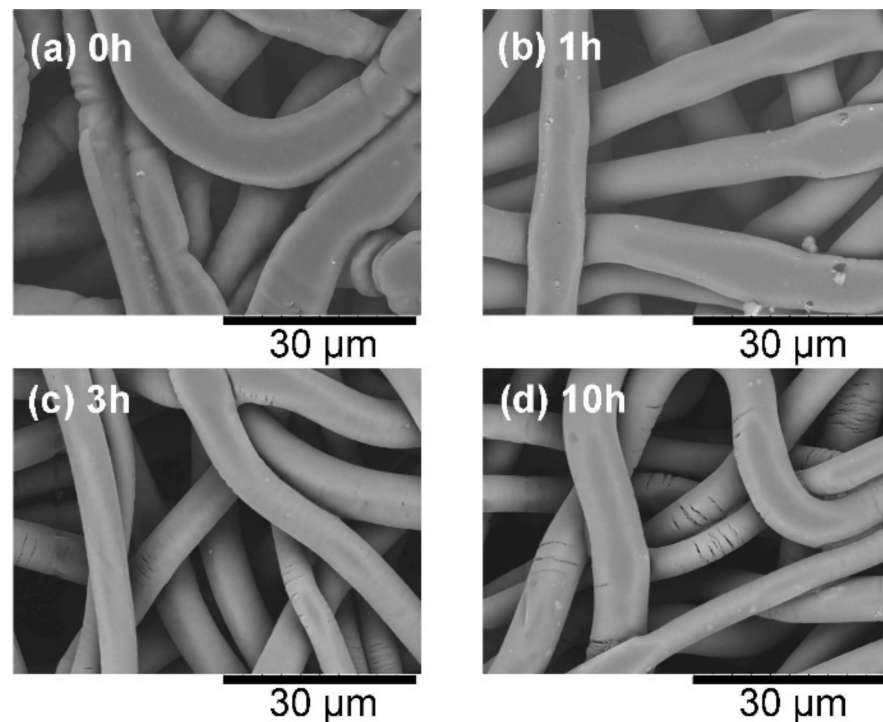


Figure 6. Scanning electron microscope images of the surfaces of CAPC products formed from (a) raw fabric, and fabric treated at 62 °C for different times: (b) 1 h, (c) 3 h, and (d) 10 h.

4. Conclusions

The CAPC method is an energy-saving resin bonding technology that belongs to the CCU category of production methods. CAPC method effectively processing fibers of a

bioplastic material (PLA) was demonstrated. Fibers with different degrees of crystallinity were prepared by heat treatment at the same temperature for different times, and their compression ratios after CO₂ exposure were compared. The fibers with a shorter heat-treatment time were more compressed than those with a long heat-treatment time and were more plasticized by CO₂. After 10 h of treatment at 62 °C, the fibers had a crystallinity of 0.17 and were cracked by the CAPC treatment; therefore, they were not suitable for this method. In contrast, the PLA fibers with low crystallinity were successfully processed using the CAPC method. Thus, it was strongly suggested that the CAPC process should be applied to fibers with low crystallinity. In some cases, PLA products are shipped after annealing to improve their thermal stability. However, unannealed PLA nonwoven fabrics with low crystallinity should be used as raw materials for CAPC.

Funding: This research received no external funding.

Data Availability Statement: All data generated or analyzed during this study are included in this published article.

Conflicts of Interest: The author declares no conflict of interest.

References

1. UN OWG. Introduction to the Proposal of the Open Working Group for the Sustainable Development Goals. *Outcome Document as of 19.6.2014 (Online)*. 2014. Available online: <https://sdgs.un.org/> (accessed on 13 April 2021).
2. Shogren, R.; Wood, D.; Orts, W.; Glenn, G. Plant-based materials and transitioning to a circular economy. *Sustain. Prod. Consum.* **2019**, *19*, 194–215. [[CrossRef](#)]
3. Inamuddin. *Green Polymer Composites Technology: Properties and Applications*; CRC Press: Boca Raton, FL, USA, 2019; ISBN 978-0367872557.
4. Sin, L.T.; Tuen, B.S. *Poly(lactic Acid): A Practical Guide for the Processing, Manufacturing, and Applications of PLA*, 2nd ed.; William Andrew: Oxford, UK, 2019; ISBN 978-0128144725.
5. Rojas, A.; Velásquez, E.; Garrido, L.; Galotto, M.J.; de Dicastillo, C.L. Design of active electrospun mats with single and core-shell structures to achieve different curcumin release kinetics. *J. Food Eng.* **2020**, *273*, 109900. [[CrossRef](#)]
6. Velásquez, E.; Vidal, C.P.; Rojas, A.; Guarda, A.; Galotto, M.J.; de Dicastillo, C.L. Natural antimicrobials and antioxidants added to polylactic acid packaging films. Part I: Polymer processing techniques. *Compr. Rev. Food Sci. Food Saf.* **2018**, *16*. [[CrossRef](#)]
7. Aizawa, T. A new method for producing porous polymer materials using carbon dioxide and a piston. *J. Supercrit. Fluids* **2018**, *133*, 38–41. [[CrossRef](#)]
8. Koysoumpa, E.K.; Bergins, C.; Kakaras, E. The CO₂ economy: Review of CO₂ capture and reuse technologies. *J. Supercrit. Fluids* **2018**, *132*, 3–16. [[CrossRef](#)]
9. Aizawa, T. Fabrication of porosity-controlled polyethylene terephthalate porous materials using a CO₂-assisted polymer compression method. *RSC Adv.* **2018**, *8*, 3061–3068. [[CrossRef](#)]
10. Aizawa, T. Peel and penetration resistance of porous polyethylene terephthalate material produced by CO₂-assisted polymer compression. *Molecules* **2019**, *24*, 1384. [[CrossRef](#)]
11. Aizawa, T.; Wakui, Y. Correlation between the porosity and permeability of a polymer filter fabricated via CO₂-assisted polymer compression. *Membranes* **2020**, *10*, 391. [[CrossRef](#)]
12. Wakui, Y.; Aizawa, T. Analysis of sustained release behavior of drug-containing tablet prepared by CO₂-assisted polymer compression. *Polymers* **2018**, *10*, 1405. [[CrossRef](#)]
13. Aizawa, T. Process development of CO₂-assisted polymer compression for high productivity: Improving equipment and the challenge of numbering-up. *Technologies* **2019**, *7*, 39. [[CrossRef](#)]
14. Aizawa, T. Novel strategy for fabricating multi-layer porous membranes with varying porosity. *ACS Omega* **2020**, *5*, 24461–24466. [[CrossRef](#)] [[PubMed](#)]
15. Aizawa, T. New design method for fabricating multilayer membranes using CO₂-assisted polymer compression process. *Molecules* **2020**, *25*, 5786. [[CrossRef](#)]
16. Kemmere, M.F.; Meyer, T. *Supercritical Carbon Dioxide in Polymer Reaction Engineering*; Wiley-VCH: Weinheim, Germany, 2005; ISBN 978-3527607051.
17. Li, M.; Zhang, J.; Zou, Y.; Wang, F.; Chen, B.; Guan, L.; Wu, Y. Models for the solubility calculation of a CO₂/polymer system: A review. *Mater. Today Commun.* **2020**, *25*, 1012772. [[CrossRef](#)]
18. Lee, J.K.; Yao, S.X.; Li, G.M.; Jun, M.B.G.; Lee, P.C. Measurement methods for solubility and diffusivity of gases and supercritical fluids in polymers and its applications. *Polym. Rev.* **2017**, *57*, 695–747. [[CrossRef](#)]
19. Gangapurwala, G.; Vollrath, A.; De San Luis, A.; Schubert, U.S. PLA/PLGA-based drug delivery systems produced with supercritical CO₂-A green future for particle formulation? *Pharmaceutics* **2020**, *12*, 1118. [[CrossRef](#)] [[PubMed](#)]

20. Villamil Jiménez, J.A.; Le Moigne, N.; Bénézet, J.-C.; Sauceau, M.; Sescousse, R.; Fages, J. Foaming of PLA composites by supercritical fluid-assisted processes: A review. *Molecules* **2020**, *25*, 3408. [[CrossRef](#)] [[PubMed](#)]
21. Balaban, M.O.; Ferrentino, G. *Dense Phase Carbon Dioxide: Food and Pharmaceutical Applications*; Wiley-Blackwell: Ames, IA, USA, 2012; ISBN 978-0813806495.
22. Drabek, J.; Zatloukal, M. Meltblown technology for production of polymeric microfibers/nanofibers: A review. *Phys. Fluids* **2019**, *31*, 091301. [[CrossRef](#)]
23. Bruckmoser, K.; Resch, K. Effect of processing conditions on crystallization behavior and mechanical properties of poly(lactic acid) staple fibers. *J. Appl. Polym. Sci.* **2015**, *132*, 42432. [[CrossRef](#)]
24. Fried, J.R. *Polymer Science and Technology*, 3rd ed.; Prentice Hall: Upper Saddle River, NJ, USA, 2014; ISBN 978-0137039555.
25. Lim, L.-T.; Auras, R.; Rubino, M. Processing technologies for poly(lactic acid). *Prog. Polym. Sci.* **2008**, *33*, 820–852. [[CrossRef](#)]
26. Young, R.J.; Lovell, P.A. *Introduction to Polymers*, 3rd ed.; CRC Press: Boca Raton, FL, USA, 2011; ISBN 978-0849339295.
27. Tomasko, D.L.; Li, H.; Liu, D.; Han, X.; Wingert, M.J.; Lee, L.J.; Koelling, K.W. A review of CO₂ applications in the processing of polymers. *Ind. Eng. Chem. Res.* **2003**, *42*, 6431–6456. [[CrossRef](#)]
28. Lian, Z.; Epstein, S.A.; Blenk, C.W.; Shine, A.D. Carbon dioxide-induced melting point depression of biodegradable semicrystalline polymers. *J. Supercrit. Fluids* **2006**, *39*, 107–117. [[CrossRef](#)]